Channels of Potential Energy Dissipation during Multiply Charged Argon-Ion Bombardment of Copper

D. Kost, S. Facsko, and W. Möller*

Institute of Ion Beam Physics and Materials Research, Forschungszentrum Dresden-Rossendorf, 01314 Dresden, Germany

R. Hellhammer and N. Stolterfoht

Division of Structure Research, Hahn-Meitner Institute, 14109 Berlin, Germany

(Received 8 January 2007; published 1 June 2007)

The dissipation of potential energy of multiply charged Ar ions incident on Cu has been studied by complementary electron spectroscopy and calorimetry at charge states between 2 and 10 and kinetic energies between 100 eV and 1 keV. The emitted and deposited fractions of potential energy increase at increasing charge state, showing a significant jump for charge states $q > 8$ due to the presence of L-shell vacancies in the ion. Both fractions balance the total potential energy, thus rendering former hypotheses of a significant deficit of potential energy obsolete. The experimental data are reproduced by computer simulations based on the extended dynamic classical-over-the-barrier model.

DOI: 10.1103/PhysRevLett.98.225503 PACS numbers: 61.80.Jh, 41.75.Ak, 52.50.Gj, 79.20.Rf

In 1983, Datz stated [1] that ''our community is almost certainly on the verge of discovering new phenomena that occur in multiply charged ion (MCI) interaction with solids.'' Since then, research is continuously verifying this statement by demonstrating not only new aspects of atomic physics which occur during the approach of an MCI to a solid surface, but also characteristic new effects of ion-solid interaction (for reviews, see Refs. [2–4]). The latter include enhanced secondary-electron emission, enhanced sputtering, and desorption of adatoms, pointing to promising prospects of MCI applications in materials science. These include surface analysis, the synthesis of materials with new properties [5,6], and the formation of nanotopographical structures on surfaces [4,7]. The effects are related to the potential energy of the MCI (the sum of the binding energies of the removed electrons), which may exceed the kinetic energy of the ion significantly at sufficiently low velocity. During MCI interaction with a solid surface, the potential energy is released in connection with the neutralization of the ion. According to the classical-over-the-barrier model [8], the interaction process may start already a few tenths of a nanometer in front of the surface, being associated with the transfer of a large number of electrons. Emission of Auger electrons from the resulting hollow atom or during its subsequent collisional interaction with the top surface [8–10] may reemit a significant fraction of the initial potential energy into the vacuum. However, this fraction plus the energy carried away by x rays and secondary atoms and ions was found to amount to less than about 10% of the initial potential energy ([11] and references therein). Thus, a substantial fraction will remain in the bulk of the substrate, which is simultaneously a prerequisite for significant effects of potential energy surface modifications.

To the best of our knowledge, only two earlier publications described measurements of this retained fraction of the potential energy. Schenkel *et al.* [11] employed a silicon detector to determine the charge transported by Auger electrons into the depletion layer as well as the charge created there by UV photons and x rays. Their result of 35%–40% of retained potential energy for highly charged Xe and Au ions represents a lower estimate as a significant fraction might be deposited in the 50 nm insensitive surface layer of their detector. Alternatively, Kentsch *et al.* [12] used a calorimetric setup to measure the retained potential energy for Ar ions incident on copper. Again, a retained fraction of 30%–40% was found, which, in comparison to Ref. [11], was considered to be fortuitous but to corroborate the conclusion that a significant fraction of the potential energy dissipates into unknown channels. Therefore, it was the aim of the present study to remeasure electron emission and calorimetric data under improved experimental conditions using the identical system of Ar^{q+} incident on copper. As we will show below, electron emission and thermalization in the solid represent the dominant channels of dissipation of potential energy. The findings are consistent with a full detection of the potential energy, thus resolving the former puzzle of unknown dissipation channels.

The electron emission experiments were performed in a UHV vacuum chamber attached to the 14.5 GHz electron cyclotron resonance (ECR) source at Hahn-Meitner Institute. The base vacuum was well in the 10^{-10} mbar range. Prior to the measurements, the polycrystalline copper samples were sputter cleaned by 3 keV Ar^+ bombardment. During the subsequent measurements of electron emission, no traces of any C or O contaminants were visible in the energy spectra. Using a deceleration lens system, the measurements were performed at fixed kinetic ion energy of 720 eV for all charge states. The available charge states were limited to $q < 10$, as the $^{40}Ar^{10+}$ beam was contaminated by ions of equal mass to charge ratio

(e.g., $^{16}O^{4+}$). To evaluate the amount of the emitted secondary-electron energy, double differential electron spectroscopy was employed yielding the number of electrons $d^2N/dEd\Omega$ per interval of electron energy E and emission angle Θ with respect to the surface normal. The data were fitted using the function [10,13]

$$\frac{d^2N}{dEd\Omega}(E,\Theta) = A(E) + B(E)\cos(\Theta), \quad (1)$$

where the fit parameters A and B were found to be essentially independent of the emission angle. The total number of electrons emitted per energy interval dN/dE is then obtained by integrating Eq. (1) over the backward 2π solid angle. Figure 1 shows the integrated electron energy spectra for different charge states of the projectiles. In addition to a pronounced low-energy fraction, a characteristic peak structure around 200 eV appears for the highest charge states. This is attributed to LMM–Auger-electron transitions, which arise for Ar^{9+} and metastable Ar^{8+} due to a vacancy in the L shell.

The total emitted energy is calculated according to

$$E^{em} = \int_E E\frac{dN}{dE}dE. \quad (2)$$

The result is shown in Fig. 2. There is a clear increase of the emitted energy at increasing charge state q of the projectile. For $q = 2$, the total amount of emitted energy is very small, which indicates that kinetic electron emission can be neglected under the present experimental conditions.

For the calorimetric measurement of the deposited potential energy, the setup at Forschungszentrum Dresden-Rossendorf [12] was considerably improved. A UHV chamber with a base pressure of $(2–3) \times 10^{-10}$ mbar, equipped with a device for vacuum sample transfer, was connected to a 14.5 GHz ECR source with a similar beam deceleration system as described above. By installing proper thermal radiation shields, the drift caused by variations of the environmental temperature was largely suppressed. During former studies [12], the ion current was measured in a separate Faraday cup with secondary-electron suppression, which might have led to errors due to the influence of the suppressor voltage on the trajectories of the low-energy ions. This procedure also required very high beam stability during the measurements. Therefore, in the present study the ion current was measured simultaneously with the calorimetric measurements. No voltage was applied to the target, while measuring the secondary-electron current at a surrounding metallic shield.

As in the former setup, the calorimeter was calibrated using an electrical reference heater. After a target cleaning procedure, as described above for the electron emission measurements, the calorimetric runs were performed at kinetic energies varying from 100 to 1000 eV for each charge state. As described in Ref. [12], the deposited fraction of the potential energy is obtained by extrapolation to zero kinetic impact energy. The results are shown in Fig. 2 for charge states ranging from 2 to 10. It should be noted that the reproducibility of the measurement (see the repeated runs at $q = 4$ and $q = 6$) is much better than the spread indicated by the error bars, which include systematic experimental errors.

Also included in Fig. 2 are the total potential energies associated with the different charge states, which have been obtained by summing over the ionization energies resulting from atomic structure codes [14,15]. Their trend of a strong increase with increasing charge state is repro-

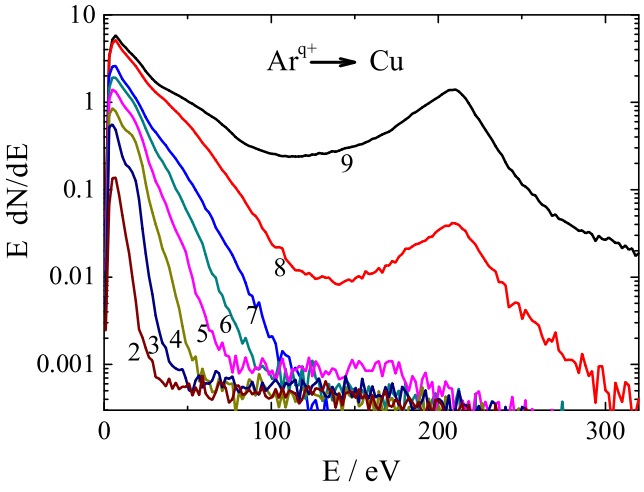

FIG. 1 (color online). Energy dispersive emitted amount of kinetic energy of secondary electrons for different charge states of argon ions impinging on a copper surface. The kinetic energy of the ions was fixed to 720 eV for all charge states.

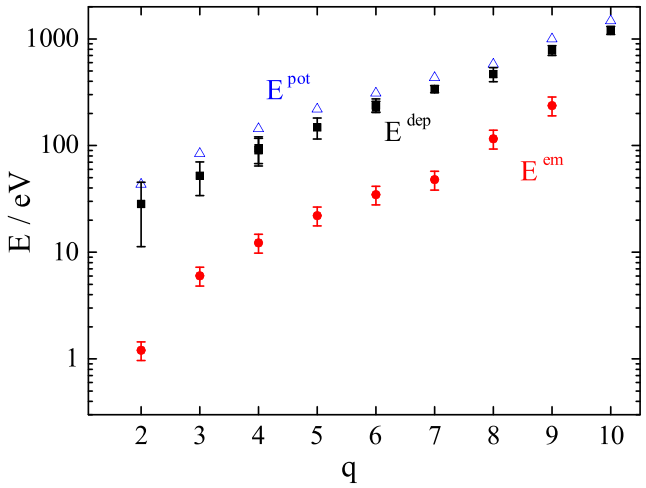

FIG. 2 (color online). Total amount of emitted electron energy E^{em} (circles) and potential energy deposited in the bulk E^{dep} (squares) per incident ion versus the charge state q of the incident argon ions. The data are compared to the potential energies E^{pot} as obtained from atomic structure codes [14,15] (open triangles).

duced by both the reemitted and the deposited fractions at a high degree of qualitative similarity. In Fig. 3, the data are replotted as fractions of the total potential energy of the projectiles. Within the experimental errors which are significant, in particular, for the low charge states, the deposited fraction is nearly constant at $(80 \pm 10)\%$. This is about twice the value of Kentsch *et al.* [12], which we mainly attribute to the improved procedure of ion current measurement. The emitted fraction amounts to $(10 \pm 5)\%$ in rough agreement with former findings [11], with a tendency of an increase at increasing charge state. The latter becomes apparent especially for charge states higher than $q = 7$ due to the onset of LMM–Auger-electron emission as described above. For the lowest charge states, the emitted fraction is somewhat underestimated, since the corresponding spectra are dominated by low-energy electrons, which are affected by a loss of detector efficiency (see Fig. 1). However, this error is small as it can be demonstrated by extrapolating the electron energy distributions towards zero energy. The sum of the results of the two complementary measurements yields a relative amount of potential energy of $(90 \pm 11)\%$ which fulfils the potential energy balance within the experimental errors. This finding is in agreement with expectation. For the present projectiles with a nuclear charge of $Z = 18$ and a highest charge state of $q = 10$, x-ray emission during the relaxation processes can be neglected, being lower by about 2 orders of magnitudes as compared to the Auger-electron yield [16–19]. Moreover, potential emission of atoms has not been

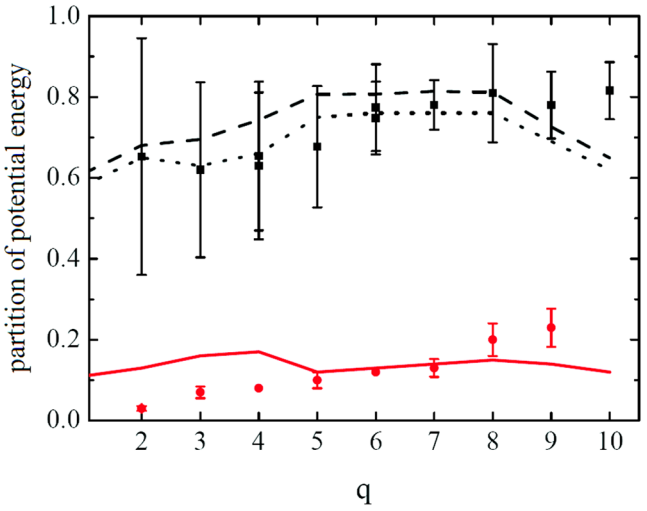

FIG. 3 (color online). Fractions of the potential energy dissipated into electron emission (circles, solid line) and deposited in the surface (squares, dashed line) versus charge state q. The symbols denote the experimental data. The lines have been obtained from numerical simulations using the extended dynamic classical-over-the-barrier model at a kinetic ion energy of 720 eV, as described in the text. The dotted line denotes the deposited fraction with the contribution from image charge acceleration being neglected.

observed for metals. Thus, the essential energy dissipation channels are secondary-electron emission and the deposition of potential energy in the subsurface atomic layers.

For corresponding calculations of the conversion of the potential energy into the dissipation channels, numerical computer simulations based on the extended dynamical classical-over-the-barrier model [8,20,21] were performed. The original simulations were mainly developed to model the relaxation of hollow atoms above the surface, whereas corresponding subsurface studies are limited [22]. Here, we extended the concepts of Refs. [20,21] for electron transfer dynamics to the subsurface regions. In brief, the processes of resonant capture and loss are switched off after crossing the jellium edge of the surface, so that the electron transfer dynamics are governed by peeloff and sidefeeding. Ion stopping in the bulk was implemented. At the instant of each Auger-electron emission the kinetic energy of the electron and the position of the ion are stored. If the ion is positioned above the surface, it is assumed that 50% of the electrons are ejected each toward the surface and away from the surface. If the electron emission takes place below the surface, we at first share the number of electrons again equally. The half that moves in the forward direction deposits all its kinetic energy in the solid. The second half, which is traveling towards the surface, is subject to electron attenuation with a probability $K(E_0, x_i)$ depending on the initial kinetic energy E_0 and the emission depth x_i of the electrons [23]. From these numbers of electrons, the fractions of energy which are deposited in the bulk or emitted into the vacuum are obtained by multiplying with the corresponding initial energies.

During the calculations, the image charge acceleration of the MCI in front of the surface is also evaluated, which, due to the low velocity of the ions, is nearly completely deposited into nuclear stopping. Thus, by means of the simulations, the fractions of potential energy deposited into the electronic and the nuclear system of the solid can be separated. The simulation results confirm that the energy required for the image charge acceleration is balanced by a shift of the atomic levels of the ion approaching the surface, i.e., fed by the potential energy of the MCI. For the present system, the image potential energy gain fraction amounts to about 5% of the total potential energy. This energy gain also contributes to the calorimetric measurement of the deposited fraction of the potential energy.

The results of the numerical calculations are given by the lines in Fig. 3. With respect to the experimental error bars, the potential energy dissipation does not significantly depend on the kinetic energy in the range of the experiments, so that the results at 720 eV are taken as being representative. Despite the simplicity of the model, a surprisingly good agreement is found between the calculated and experimental data. The calculated emitted fraction is in good quantitative agreement with the experiments in aver-

age, but is almost independent of the charge state in contrast to the experimental trend. For the deposited fraction, there is a significant deviation only at the highest charge states. The model calculations treat the influence of the image charge potential on the atomic levels of the ions as a perturbation. For L-shell vacancies, the ion neutralization in front of the surface is reduced due to frequent autoionization processes, so that the ion survives longer when approaching the surface. This leads to an increase of the perturbation and a correspondingly reduced energy of the released electrons. As the screening by outer electrons is neglected, this high perturbation might be partly artificial and result in a reduced calculated fraction of the released potential energy.

Both in experiment and from calculation, the deposited and emitted fractions do not fully add to the nominal potential energy of the ions. The latter is given relative to the vacuum level, whereas during ion-solid interaction electrons are transferred to the ion from the Fermi level of the solid, which corresponds to the consumption of the work function per transferred electron. With the work function of Cu of 4.4 eV, this energy consumption ranges from about 10 to 40 eV for the present charge states. At the charge states of 6 and 7, where the experimental errors are relatively small and the agreement between model calculations and experiments is best (see Fig. 3), the resulting relative energy deficit is about 8% in good agreement with the data of Fig. 3. This, however, might be fortuitous in view of the experimental errors and the simplicity of the model.

Summarizing, we conclude that the potential energy of the MCI is released by emission of a specific number of Auger electrons along the ion trajectory, which either are emitted into the vacuum or deposit their kinetic energy in the solid, depending on the MCI position at emission time and the energy of the Auger-electron transition. For the first time, it is demonstrated that the fraction of the potential energy of multiply charged ions which is released by Auger electrons, and the fraction which is deposited into the target, balance with the total potential energy at different charge states. For argon ions incident on copper with charge states up to 10, the deposited fraction is almost independent of the charge state. The results of computer simulations based on the extended dynamic classical-over-the-barrier model are in good agreement with the experimental data, thus corroborating the picture that the potential energy is essentially transferred via Auger electrons, which are either emitted into the vacuum or deposited into the bulk.

*Corresponding author.
Email address: w.moeller@fzd.de
Fax: +49-351-260 3285

[1] S. Datz, Phys. Scr. **T3**, 79 (1983).
[2] A. Arnau *et al.*, Surf. Sci. **27**, 113 (1997).
[3] J. D. Gillaspy, J. Phys. B **34**, R93 (2001).
[4] F. Aumayr and H. P. Winter, Nucl. Instrum. Methods Phys. Res., Sect. B **233**, 111 (2005).
[5] G. Borsoni *et al.*, Solid-State Electron. **46**, 1855 (2002).
[6] T. Meguro *et al.*, Nucl. Instrum. Methods Phys. Res., Sect. B **235**, 431 (2005).
[7] M. Terada *et al.*, Nucl. Instrum. Methods Phys. Res., Sect. B **235**, 452 (2005).
[8] J. Burgdörfer, P. Lerner, and F. Meyer, Phys. Rev. A **44**, 5674 (1991).
[9] F. Aumayr *et al.*, Phys. Rev. Lett. **71**, 1943 (1993).
[10] R. Köhrbrück *et al.*, Phys. Rev. A **45**, 4653 (1992).
[11] T. Schenkel *et al.*, Phys. Rev. Lett. **83**, 4273 (1999).
[12] U. Kentsch, H. Tyrroff, G. Zschornack, and W. Möller, Phys. Rev. Lett. **87**, 105504 (2001).
[13] R. Köhrbrück *et al.*, Phys. Rev. A **50**, 1429 (1994).
[14] R. D. Cowan, *The Theory of Atomic Structure and Spectra* (University of California Press, Berkeley, 1981).
[15] M. F. Gu, Astrophys. J. **582**, 1241 (2003).
[16] G. Wenzel, Z. Phys. **43**, 524 (1927).
[17] K. D. Sevier, *Low Energy Electron Spectrometry* (John Wiley & Sons, New York, 1972).
[18] R. W. Fink, R. C. Jopson, H. Mark, and C. D. Swift, Rev. Mod. Phys. **38**, 513 (1966).
[19] G. D. Archard, in *Proceedings of the Second International Symposium on X-Ray Microscopy and Microanalysis, Stockholm, 1959* (Elsevier, Amsterdam, 1960).
[20] J. Ducree, H. J. Andrä, and U. Thumm, Phys. Scr. **T80**, 220 (1999).
[21] J. Ducree, F. Casali, and U. Thumm, Phys. Rev. A **57**, 338 (1998).
[22] N. Stolterfoht, A. Arnau, M. Grether, R. Köhrbrück, A. Spieler, R. Page, A. Saal, J. Thomaschewski, and J. Bleck-Neuhaus, Phys. Rev. A **52**, 445 (1995).
[23] P. J. Cumpson and M. P. Seah, Surf. Interface Anal. **25**, 430 (1997).